Human iPSC-derived trigeminal neurons lack constitutive TLR3-dependent immunity that protects cortical neurons from HSV-1 infection

Bastian Zimmer[a,b,1], Osefame Ewaleifoh[c,1], Oliver Harschnitz[a,b], Yoon-Seung Lee[d,e,f], Camille Peneau[d], Jessica L. McAlpine[a,b], Becky Liu[a,b], Jason Tchieu[a,b], Julius A. Steinbeck[a,b], Fabien Lafaille[d], Stefano Volpi[g], Luigi D. Notarangelo[h], Jean-Laurent Casanova[d,e,f,i,j,2], Shen-Ying Zhang[d,e,f,1], Gregory A. Smith[c,1,2], and Lorenz Studer[a,b,1,2]

[a]Center for Stem Cell Biology, Sloan Kettering Institute for Cancer Research, New York, NY 10065; [b]Developmental Biology Program, Sloan Kettering Institute for Cancer Research, New York, NY 10065; [c]Department of Microbiology-Immunology, Northwestern University Feinberg School of Medicine, Chicago, IL 60611; [d]St. Giles Laboratory of Human Genetics of Infectious Diseases, Rockefeller Branch, The Rockefeller University, New York, NY 10065; [e]Laboratory of Human Genetics of Infectious Diseases, Necker Branch, Necker Hospital for Sick Children, 75015 Paris, France; [f]Imagine Institute, Paris Descartes University, 75015 Paris, France; [g]Pediatric and Rheumatology Unit, Center for Autoinflammatory Diseases and Immunodeficiencies, Istituto Giannina Gaslini and University of Genoa, 16147 Genoa, Italy; [h]Laboratory of Clinical Immunology and Microbiology, National Institute of Allergy and Infectious Diseases, National Institutes of Health, Bethesda, MD 20892; [i]Howard Hughes Medical Institute, The Rockefeller University, New York, NY; and [j]Pediatric Hematology-Immunology Unit, Necker Hospital for Sick Children, 75015 Paris, France

Contributed by Jean-Laurent Casanova, July 30, 2018 (sent for review June 19, 2018; reviewed by Lynn W. Enquist and Marius Wernig)

Herpes simplex virus type 1 (HSV-1) encephalitis (HSE) is the most common sporadic viral encephalitis in Western countries. Some HSE children carry inborn errors of the Toll-like receptor 3 (TLR3)-dependent IFN-α/β– and -λ–inducing pathway. Induced pluripotent stem cell (iPSC)-derived cortical neurons with TLR3 pathway mutations are highly susceptible to HSV-1, due to impairment of cell-intrinsic TLR3-IFN immunity. In contrast, the contribution of cell-intrinsic immunity of human trigeminal ganglion (TG) neurons remains unclear. Here, we describe efficient in vitro derivation and purification of TG neurons from human iPSCs via a cranial placode intermediate. The resulting TG neurons are of sensory identity and exhibit robust responses to heat (capsaicin), cold (icilin), and inflammatory pain (ATP). Unlike control cortical neurons, both control and TLR3-deficient TG neurons were highly susceptible to HSV-1. However, pretreatment of control TG neurons with poly(I:C) induced the cells into an anti–HSV-1 state. Moreover, both control and TLR3-deficient TG neurons developed resistance to HSV-1 following pretreatment with IFN-β but not IFN-λ. These data indicate that TG neurons are vulnerable to HSV-1 because they require preemptive stimulation of the TLR3 or IFN-α/β receptors to induce antiviral immunity, whereas cortical neurons possess a TLR3-dependent constitutive resistance that is sufficient to block incoming HSV-1 in the absence of prior antiviral signals. The lack of constitutive resistance in TG neurons in vitro is consistent with their exploitation as a latent virus reservoir in vivo. Our results incriminate deficiencies in the constitutive TLR3-dependent response of cortical neurons in the pathogenesis of HSE.

HSE | TG neurons | HSV-1 | TLR3 | antiviral immunity

Herpes simplex virus 1 (HSV-1) is a double-stranded DNA virus that infects about 80% of humans world-wide by the age of 20 y, mainly following interhuman transmission by saliva (1). The virus infects via the oral or nasal epithelium (2). Primary infection can be asymptomatic or manifest as gingivostomatitis, and is typically followed by viral latency in trigeminal ganglion (TG) neurons. HSV-1 exhibits an unusual form of neurotropism; the virus is highly neuroinvasive, but for unknown reasons infection is typically restricted to sensory and autonomic neurons of the peripheral nervous system (PNS) and rarely involves the central nervous system (CNS). Viral reactivation from latency can manifest as herpes labialis, which is common in the general population and in most cases is self-healing. Rare patients, typically children, develop HSV-1 encephalitis (HSE) in the course of primary infection (3, 4).

HSE is the most common sporadic viral encephalitis of childhood in the Western world (5). If untreated, HSE has a high mortality rate, and acyclovir-treated survivors often suffer from profound long-term neurological sequelae (6). The virus reaches the CNS, likely via the olfactory nerve and olfactory bulb, to affect the temporal and frontal lobes of the brain. Less frequently, the virus can reach the CNS via other peripheral routes, such as the TG nerve (sensory) and the superior cervical and parasympathetic ganglia (autonomic), which are particularly associated with HSE in the brainstem (7). Whereas many neurotropic pathogens reach the CNS by breaching the blood–brain barrier, HSV-1 and related alphaherpesviruses are among the very few viruses that invade the CNS by trafficking through neural

Significance

We previously demonstrated that induced pluripotent stem cell (iPSC)-derived cortical neurons from HSV-1 encephalitis patients with Toll-like receptor 3 (TLR3) pathway deficiencies are highly susceptible to HSV-1, due to impairment of cell autonomous TLR3-IFN immunity. In this study we present a protocol for efficient derivation/purification of trigeminal ganglion (TG) neurons from human iPSCs. The resulting TG neurons are of sensory identity and exhibit robust biological function. We also show that TG neurons and cortical neurons play distinct roles in host defense against HSV-1 in the central nervous system: unlike cortical neurons, TG neurons are vulnerable to HSV-1 because they require preemptive induction of TLR3-, IFN-α/β–mediated immunity. This is an important step to further our understanding of the HSV-1 encephalitis disease mechanism.

Author contributions: B.Z., O.E., O.H., L.D.N., J.-L.C., S.-Y.Z., G.A.S., and L.S. designed research; B.Z., O.E., O.H., Y.-S.L., C.P., J.L.M., B.L., J.T., J.A.S., F.L., S.V., and S.-Y.Z. performed research; B.Z., O.E., O.H., L.D.N., S.-Y.Z., G.A.S., and L.S. analyzed data; and B.Z., O.E., O.H., L.D.N., J.-L.C., S.-Y.Z., G.A.S., and L.S. wrote the paper.

Reviewers: L.W.E., Princeton University; and M.W., Stanford University.

Conflict of interest statement: L.W.E. and G.A.S. are coauthors on a 2017 paper [Pomeranz LE (2017) *J Neurosci* 37:4128–4144], in which they independently provided unpublished reagents/analytic tools.

[1]B.Z., O.E., S.-Y.Z., G.A.S., and L.S. contributed equally to this work.

[2]To whom correspondence may be addressed. Email: casanova@rockefeller.edu, g-smith3@northwestern.edu, or studerl@mskcc.org.

This article contains supporting information online at www.pnas.org/lookup/suppl/doi:10.1073/pnas.1809853115/-/DCSupplemental.

Published online August 28, 2018.

circuits of the PNS. The fundamental question of why HSV-1 normally infects the PNS but not the CNS, and the relationship between breakdown of this differential neurotropism and the development of HSE remain long-standing challenges in the field (8).

The generation of induced pluripotent stem cells (iPSCs) from human fibroblasts (9, 10) has enabled the development of patient-specific in vitro disease models (11). A key requirement for such studies is the derivation of disease-relevant cell types, such as specific neurons of CNS and PNS identity. Protocols have been developed for the directed differentiation of human iPSCs into various neuronal lineages of the CNS (12). Access to defined human PNS lineages from embryonic stem cells (ESCs) or iPSCs has been more limited and includes the derivation of dorsal root ganglia (DRG)-type sensory (13) or, more recently, enteric neuronal lineages (14). Human sensory neurons have been used to model human pain (15) and to test drug toxicity (16). A sensory lineage of particular importance are TG neurons, which are involved in the pathogenesis of trigeminal neuralgia, one of the most severe forms of human pain, and possibly in the genesis of migraine headaches, given the prominent role of CGRP receptor signaling in the TG (17). TG neurons also play a prominent role during HSV-1 infection as a site of viral latency and as a potential portal of entry to the CNS in cases of brainstem HSE.

We previously found that children with single-gene inborn errors of Toll-like receptor 3 (TLR3)-dependent IFN-α/β– or -λ–mediated immunity are prone to HSE (18–23). TLR3 is one of several receptors that can be activated by viral or cellular double-stranded RNA (dsRNA) (24), and the sole known receptor located along the secretory pathway where it can detect luminal, as opposed to cytosolic dsRNA. UNC-93B is a membrane-bound protein essential for TLR3 signaling (18). We also found that HSV-1 replicated at higher levels in TLR3-deficient and UNC93B-deficient CNS cortical neurons derived from patient-specific iPSCs, compared with control neurons (25). Moreover, the production of IFNs in TLR3-deficient neurons was impaired in response to both HSV-1 and the TLR3 nonspecific agonist poly(I:C), which mimics dsRNA. These results suggested that defects of cell-intrinsic immunity to HSV-1 in cortical neurons may underlie HSE in patients with mutations in the TLR3 signaling pathway. However, it remained unclear whether PNS neurons deficient for TLR3 exhibit increased susceptibility to HSV-1 and thereby also contribute to HSE pathogenesis. In the present study we address this question experimentally.

Results

Differentiation of Human iPSCs and ESCs into TG Neurons Under Defined Xeno-Free Conditions. We recently reported the differentiation of human pluripotent stem cells (hPSCs: referring to both human ESCs and iPSCs) into a cranial placode lineage under defined conditions (26). However, the conditions used to specifically generate TG placodes were based on poorly defined components, such as knockout serum replacement and mouse embryo fibroblast feeder cells (27), factors that likely increase technical variability in iPSC-based disease modeling studies. Furthermore, the published protocols (27) were inefficient and produced TG neurons of low purity that were not suitable for testing the cell-autonomous susceptibility to HSE. Therefore, we established a robust TG neuron differentiation platform based on fully defined conditions for early ectodermal lineage choice (26), and determined specific extrinsic patterning conditions to direct hPSCs into TG neuron precursors. We introduced two major changes to the earlier protocols. First, early low-dose bone marrow protein (BMP)4 exposure during placode induction (instead of transient BMP inhibition) triggered the rapid induction of BMP-dependent markers of nonneural ectoderm (27), such as AP2A and AP2C (*SI Appendix*, Fig. S1*A*). Second, exposure of the cells to the GSK3β inhibitor and WNT agonist CHIR99021 biased the regional placode identity toward PAX3 expression characteristic of the TG placode (Fig. 1*A*). Using those modified conditions, we obtained cultures of cranial placode precursors expressing SIX1 and PAX3 starting at day 4 of differentiation (*SI Appendix*, Fig. S1*A*). However, we also observed a proportion of $PAX3^+$ cells coexpressing the neural crest marker SOX10 (*SI Appendix*, Fig. S1*A*), suggesting a broader neural border identity comprising neural crest and cranial placode lineages. Interestingly, both the cranial placode and neural crest contribute to TG neuron development (28, 29). Upon further differentiation, placodal precursors maintained SIX1 expression while the percentage of $PAX3^+$ cells decreased, with PAX3 representing a transient precursor marker in both preplacode and neural crest lineages (Fig. 1*B*). The resulting neurons at day 20 and day 40 of differentiation retained SIX1 expression and coexpressed the sensory neuron marker ISL1, which is consistent with TG neuron identity (Fig. 1*C* and *SI Appendix*, Fig. S1*B*). However, our TG placode induction protocol retains a proportion of contaminating $AP2A^+$ but $SIX1^-$ surface ectoderm cells, a lineage developmentally related to the cranial placode that can give rise to keratinocyte-like cells (26, 27). Our placode induction protocol worked reliably across multiple human iPSC lines with minimal variability in yield (*SI Appendix*, Fig. S1*C*).

Identification of GD2 as a Cell Surface Marker to Purify TG Neurons in Vitro. For testing the intrinsic response to stimuli and immunity to viruses of defined neural lineages in the study of HSE, we previously established protocols to purify each of the major human iPSC-derived CNS cell types (cortical neurons, astrocytes, oligodendrocytes, or neural stem cells) at >80% purity (25). Here, we developed a similar strategy for the prospective isolation of highly enriched and developmentally synchronized human iPSC-derived TG neurons. We made use of our recently developed *SIX1::H2BGFP* knockin reporter cell line (30) to carry out a cell surface marker screen probing 242 commercially available antibodies (31) under conditions of TG placode induction (*SI Appendix*, Fig. S2). Five hits were identified (CD40, CD57, CD81, CD150, GD2) that showed a high percentage of colabeling with $SIX1::H2BGFP^+$ cells (*SI Appendix*, Fig. S3*A*). We selected the GD2 ganglioside as a surface antigen for the purification of TG neurons (Fig. 1*D*) derived from both human ESC and iPSCs based on the data from the primary screen, analysis of existing literature, and follow-up validation studies (*SI Appendix*, Fig. S3*B*). The identity of the cells was validated following FACS-based isolation of $GD2^+$ and $GD2^-$ cells by quantitative real-time (qRT)-PCR analysis (Fig. 1*E*). The $GD2^+$ fraction was enriched for the pan placodal markers SIX1 and PAX3 compared with unsorted cells. Additionally, the sensory neuron markers POU4F1 (BRN3A), PRPH (peripherin), RET, and NTRK1 (TRKA) were enriched in the $GD2^+$ versus matched unsorted cells, and were depleted in the $GD2^-$ cells.

Functional Characterization of Human iPSC-Derived TG Neurons. Further differentiation of the $GD2^+$ cells resulted in the upregulation of the three neurotrophin receptors (NTRK1, NTRK2, and NTRK3, also known as TRKA, -B, and -C, respectively). Expression of specific TRK receptors marks sensory neuron subtypes, such as pain-sensing (nociceptive), mechanoceptive, and proprioceptive lineages (32). Our data suggest the presence of TG neurons representing all three sensory modalities in the human iPSC-derived cultures (Fig. 1*F*). Furthermore, the expression of pain-related receptors, such as TRPV1 (heat; e.g., capsaicin), TRMP8 (cold; e.g., icilin), and P2RX3 [inflammatory pain; e.g., α, β-methyleneadenosine 5′-triphosphate trisodium salt (ATP)] (Fig. 1*F*) indicated the presence of various subtypes of nociceptive neurons. We used calcium imaging to demonstrate receptor function in these cells. Starting at day 30 of differentiation, calcium responses were triggered by capsaicin, icilin, and ATP

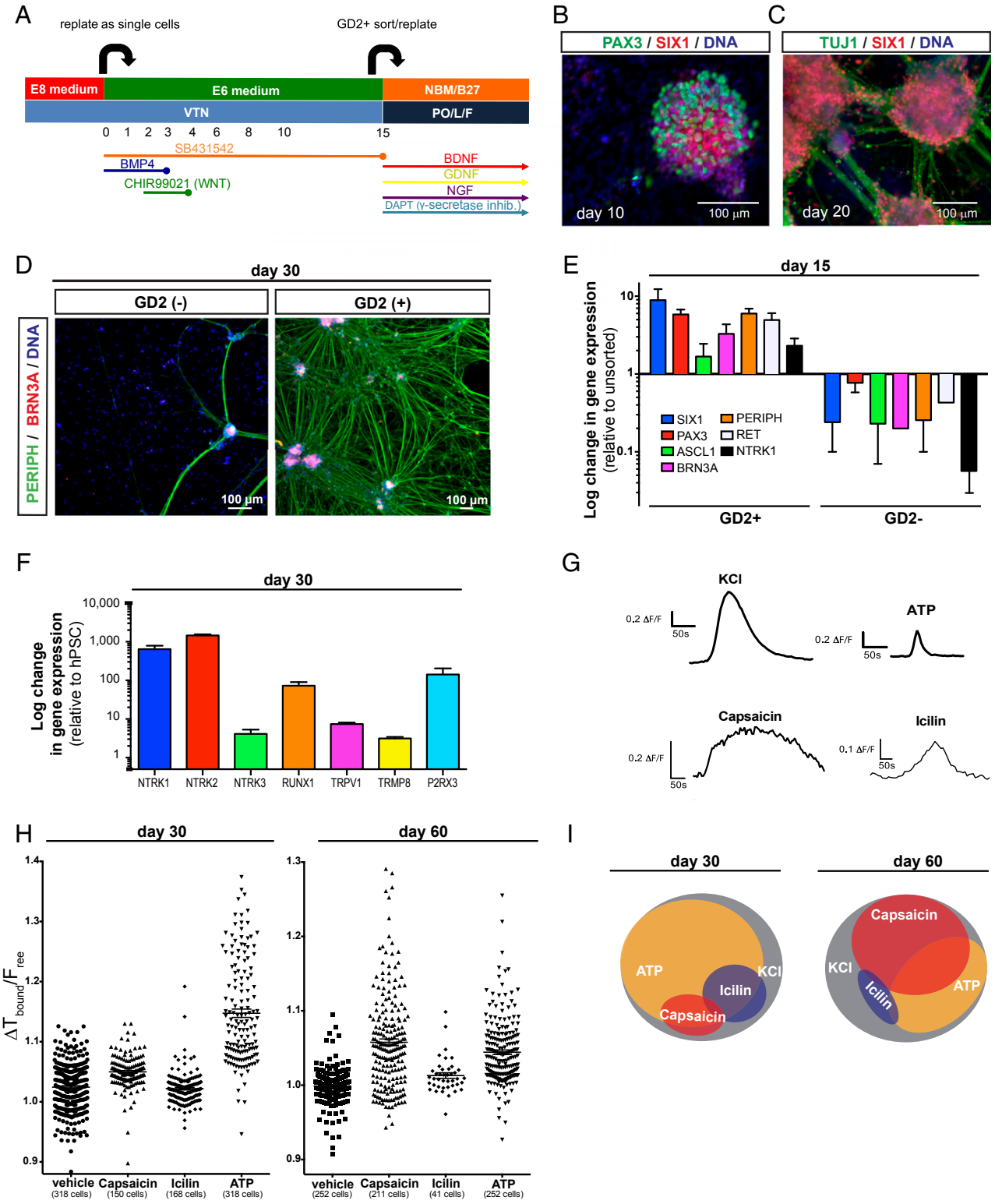

Fig. 1. Differentiation and functional characterization of trigeminal neurons derived from human iPSC under fully defined conditions. (*A*) Modified trigeminal placode induction protocol using only fully defined components. VTN, vitronectin. (*B*) Placodal clusters staining for SIX1 (cranial placode) and PAX3 (trigeminal placode) after 10 d of differentiation. (*C*) Placodal clusters rapidly differentiate into TG neurons staining positive for TUJ1 and SIX1 after 20 d of differentiation. (*D*) Sorting for GD2 on day 15 of differentiation results in highly pure TG neurons staining for peripherin and Brn3a after 15 additional days of differentiation. (*E*) Gene-expression analysis of key sensory and TG neuron markers after GD2 sorting on day 15 of differentiation. Data are expressed as fold-changes compared with unsorted cells. (*F*) Gene-expression analysis of nociceptor genes on day 30 of differentiation. (*G*) Representative individual calcium traces for the four different stimuli used. (*H*) Calcium response to capsaicin, icilin, and ATP of each individual cell analyzed on day 30 and day 60 of differentiation. (*I*) Venn diagram showing subgroups of TG neurons that respond to KCl, capsaicin, icilin, and ATP.

(Fig. 1 *G* and *H* and *SI Appendix*, Fig. S4). Additional in vitro maturation to day 60 of differentiation revealed progressive changes in subtype composition. While at day 30 of differentiation many of the cells (~70%) responded to ATP, only a small fraction responded to capsaicin (~10%) or icilin (~15%). In contrast, by day 60, the percentage of cells responding to ATP dropped to ~35%, while now ~50% of the cells reacted to capsaicin. The percentage of cells responding to icilin was slightly decreased to ~10% of total cells (Fig. 1*I*). Interestingly, maturation was also associated with a more selective response pattern. While at day 30 most of the capsaicin- or icilin-responsive cells also responded to ATP, at day 60 most cells responded to only a single stimulus. Finally, the isolation of $GD2^+$ cells at day 15 of differentiation resulted in neuronal populations at purities of >90% by day 30 of differentiation. Our data demonstrate the robust derivation of functional TG sensory neurons at very high purity.

Healthy Control and TLR3-Deficient Human iPSC-Derived TG Neurons Are Equally Permissive to HSV-1 Infection. We previously reported that human iPSC-derived CNS neurons from healthy controls are relatively resistant to HSV-1 infection and that this protection is provided by TLR3 (25). To determine the susceptibility of human iPSC-derived TG neurons to HSV-1 in culture, $TUJ1^+$ TG placode precursors were further differentiated into more mature TG neurons for 14–18 d. Human iPSC-derived TG and CNS neurons were derived in parallel from healthy controls and from an autosomal recessive (AR) complete TLR3-deficient HSE patient (33). Each cell population was infected for 20 h with an HSV-1 strain F recombinant that encoded a mCherry fluorescent protein fused to the pUL25 minor capsid protein (Fig. 2 *A* and *B*) (34). Because the fluorescence emitted from individual input virions was below the limits of detection in this assay, only nuclei filled with de novo assembled capsids were observed and scored as infected. It should be noted that this fluorescence assay measures cell susceptibility to HSV-1, as well as progression to a late stage of infection, but does not indicate whether infectious virions were released from the cells. The results in CNS neurons confirmed our previous findings that had used a GFP-capsid KOS strain of HSV-1, with a near complete resistance to HSV-1 for cells derived from healthy control iPSCs at the 24-h time point that was absent from AR complete TLR3-deficient CNS neurons (25). In contrast to the control CNS neurons, TG neurons derived from healthy control iPSCs were susceptible to HSV-1 infection at the 20-h time point, like TG neurons derived from a patient with AR complete TLR3 deficiency (Fig. 2 *A* and *B*).

TG Neurons Show More Rapid Progression of HSV-1 Infection. The susceptibility of the TG neurons to HSV-1 infection could either be due to an insufficient TLR3 response that failed to prevent infection under the experimental conditions, or the absence of a TLR3 response altogether. To resolve whether TLR3 provided a measurable degree of HSV-1 resistance to TG neurons, the expression kinetics of HSV-1 fluorescence was examined from 4- to 12-h postinfection in control and TLR3-deficient TG neurons, and TLR3-deficient CNS neurons that are also susceptible to HSV-1 infection (Fig. 2*C*). Unexpectedly, infections of control TG neurons progressed more rapidly than did TLR3-deficient CNS infection, suggesting that even in the absence of TLR3 the CNS neurons possessed greater intrinsic resistance to HSV-1 than did the control TG neurons. Furthermore, TLR3 did not substantially impact the rate of HSV-1 infection in the TG neurons, as patient and control TG populations were equally susceptible throughout the time course. The absence of TLR3-based protection from HSV-1 in the TG neurons was also observed at lower doses of HSV-1, indicating that a potential TLR3 response in control TG was not being overwhelmed by the magnitude of the HSV-1 challenge (Fig. 2*D*). Together, these results indicate that TG neurons are ineffective at restricting HSV-1, and AR complete TLR3-deficiency does not increase their susceptibility to HSV-1 infection. These results are compatible with the fact that TG neurons are susceptible to HSV-1 infection in healthy humans and demonstrate that the differential PNS/CNS neural tropism of HSV-1, typical of human infections, can be modeled with the corresponding human iPSC-derived neuronal lineages in culture.

IFN-β Antagonizes HSV-1 Infection of TG Neurons. We next asked whether TG neurons can be protected by treatment with IFN-β before HSV-1 exposure, a paradigm previously shown to protect TLR3-deficient iPSC-derived CNS neurons (25). Control TG, TLR3-deficient TG, and TLR3-deficient CNS neurons were treated with 1,000 IU/mL recombinant human IFN-β for 18 h before challenge with HSV-1, with the IFN-β maintained throughout the infection. IFN-β treatment established an antiviral state in all three populations (Fig. 2*E*). Unlike IFN-β, IFN-λ1 did not protect the neurons from HSV-1 (Fig. 2*F*), which is consistent with our previous findings in TLR3-deficient CNS neurons (25). These results confirm that an IFN-β preconditioned antiviral response protects PNS and CNS neurons, thereby showcasing the capacity of these cells to resist HSV-1. However, these elicited antiviral states did not account for the constitutive cell-intrinsic resistance to HSV-1 infection observed in control CNS neurons.

Pretreatment with Poly(I:C) Antagonizes HSV-1 Infection in Control TG Neurons. To address whether TG neurons are capable of mounting a TLR3-mediated response, the cells were stimulated with the nonspecific TLR3-agonist poly(I:C) 18 h before HSV-1 challenge. Similar to preconditioning with IFN-β, poly(I:C) induced a resistant state in the control TG neurons (Fig. 2*G*). Although the magnitude of the protection afforded by poly(I:C) pretreatment (34% of cells remained susceptible on average for the TG control sample) was less than that observed with IFN-β (19% of cells remained susceptible on average for the TG control sample) (Fig. 2*E*), we do not ascribe significance to this difference because the relative activities of the two agonists was unknown. As expected, TLR3-deficient CNS and TG neurons were not protected by poly(I:C) pretreatment. These data infer that TG neurons possess functional TLR3 receptors despite lacking the constitutive cell-intrinsic resistance observed in control CNS neurons.

IFNs and ISGs Are Induced by TLR3 Stimulation in Control TG Neurons. In fact, testing mRNA expression of 19 different IFNs and 4 different IFN stimulated genes (ISGs) by qRT-PCR showed that poly(I:C) triggered induction of at least three IFN species and four ISGs in control TG neurons, including the three subtypes of *IFNL*, *MX1*, *OAS1*, *ISG15*, and *IFIT2*, that were abolished in TLR3-deficient TG neurons (*SI Appendix*, Fig. S5). In contrast, HSV-1 infection triggered similarly weak expression of some IFN-α species in control and TLR3-deficient TGs, including at least *IFNA4*, *IFNA5*, *IFNA7*, *IFNA10*, *IFNA13*, *IFNA14*, but not the four ISGs studied (*SI Appendix*, Fig. S5). It is intriguing that the TG neuron cell-autonomus induction of *IFN* by HSV-1 was not able to render these cells resistant to HSV-1 infection, whereas exogeneous recombinant IFN-β reduced the susceptibility of TG neurons to HSV-1 (Fig. 2*E*). The limited IFN and ISG subtypes induced and the low induction levels, upon virus infection, may explain this lack of protective effect of the virus-induced IFN production. Thus, while TG neurons produce a broad IFN response following TLR3 stimulation, this induced response was ineffective at preventing HSV-1 infection in the absence of preconditioning (Fig. 2*G*). Collectively, our data establish that TG neurons, like cortical neurons, sense dsRNA via TLR3 and produce IFNs, yet lack the constitutive TLR3 response that protects cortical neurons from incoming HSV-1. The high susceptibility of the TG neurons to HSV-1 is consistent with HSV-1 routinely entering PNS neurons

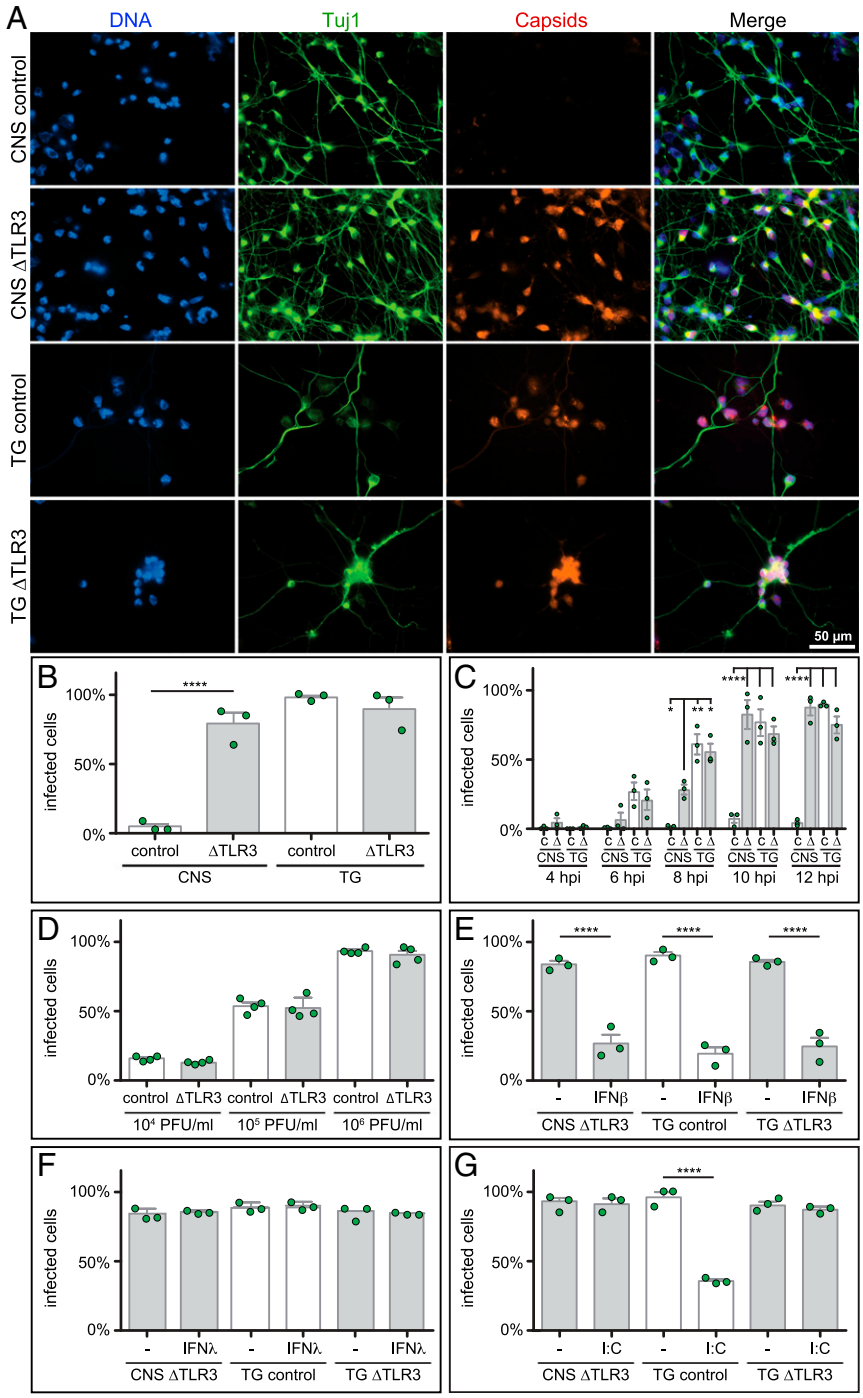

Fig. 2. CNS and PNS neuron susceptibility parallels natural human infections and is restricted by IFN and a TLR3 agonist. (*A*) Representative images of HSV-1 infection in control and AR patient (ΔTLR3) iPSC-derived neurons. Cells were infected with 5×10^6 plaque-forming units (PFU) of HSV-1 strain F encoding a pUL25/mCherry capsid reporter for 20 h before fixation and staining for chromosomes (DAPI) and a neuron-specific tubulin isoform (Tuj1). (*B*) Percentage of infected Tuj1$^+$ cells based on fluorescent capsid expression at 20-h postinfection, as in *A*. (*C*) Percentage of infected control (C) and AR patient (Δ) iPSC-derived CNS and TG neurons based on fluorescent capsid expression at the indicated times postinfection with 5×10^6 PFU. (*D*) Percentage of infected TG neurons based on fluorescent capsid expression at 20-h postinfection. Cells were exposed to the indicated amounts of the pUL25/mCherry capsid reporter strain of HSV-1. (*E*–*G*) Percentage of infected cells following 18-h pretreatment with either IFN-β (IFNβ), IFN-λ (IFNλ), or poly(I:C). Data points represent replicate experiments and error bars indicate the SEM. ****$P < 0.0001$, **$P < 0.01$, *$P < 0.1$ (one-way ANOVA).

of infected individuals, while the constitutive resistance of cortical CNS neurons is consistent with HSE being a rare complication. The loss of this previously unrecognized constitutive TLR3 CNS response mechanism in TLR3-deficient patients may underlie their increased incidence of HSE.

Discussion

TG neurons are a common portal for HSV-1 entry into the PNS. The virus establishes latency in TG neurons and subsequently reactivates to cause herpes labialis. This life-long infectious cycle notably lacks CNS involvement, and showcases the differential

neurotropism exhibited by HSV-1 and related members of the alphaherpesvirinae subfamily of viruses (35). Maintenance of HSV-1 latency is in part under the control of T cells, as evidenced by the recurrence, persistence, or severity of cutaneous lesions in patients with inherited or acquired forms of T cell deficiency (36, 37). In contrast, inborn errors of TLR3-dependent IFN immunity predispose children to HSE, not herpes labialis. These patients' T cells are intact and most leukocytes do not rely on TLR3 to detect dsRNA and viruses, including HSV-1 (19, 33). Experimental data from patient-specific iPSC-derived cortical neurons suggested that the critical role of TLR3 in the restriction of HSV-1 infection is intrinsic to the CNS neurons themselves (25). Because PNS neurons are normally targeted by HSV-1 during natural human infections, understanding the role of TLR3 in these cells is critical to deciphering the differential neurotropism of HSV-1 and its contribution to a homeostasis that normally precludes HSE. To this end, we developed an experimentally robust and chemically defined protocol for generating human iPSC-derived TG neurons, which are suitable for modeling HSV-1 infection in healthy controls and TLR3-mutated patients.

Human iPSC-derived TG neurons have enabled us to compare HSV-1 infection in PNS and CNS neurons derived from the same individuals. Remarkably, the susceptibility of iPSC-derived neurons mimics tissue susceptibility of natural infections: TG neurons are susceptible to HSV-1 infection while cortical neurons are resistant. Thus, the differential neurotropism exhibited by HSV-1 in humans in vivo is replicated in this culture model in vitro. We also identified a potential explanation for the differential neurotropism of HSV-1, as our results suggested that cortical neurons possess a TLR3-dependent, constitutive immunity to HSV-1 that is absent from TG neurons. We define this constitutive immunity as a cell-intrinsic response that antagonizes HSV-1 infection in the absence of preconditioning. Although cortical neurons uniquely possess constitutive resistance to HSV-1, both cortical and TG neurons possess inducible resistance to HSV-1. Indeed, preconditioning TLR3-deficient cortical neurons and control or TLR3-deficient TG neurons with IFN-β confers protection from HSV-1. Previous studies have noted a similar inducible paracrine antiviral effect of IFN-β in rodent TG neurons (38, 39). In control TG neurons, but not TLR3-deficient TG neurons, preconditioning with poly(I:C) also promoted an anti-HSV state, demonstrating that TLR3 is functional in these cells despite the lack of constitutive resistance.

Moreover, the poly(I:C) preconditioned response in control TG neurons included the induction of IFNs and ISGs. Autocrine effects of IFN-β, but notably not IFN-λ, may promote the antiviral state in TG neurons by amplifying ISG production, which is consistent with the effects of preconditioning with these molecules directly. However, a key finding of this study is that this inducible response did not correlate with any measurable degree of native protection from HSV-1 under the in vitro experimental conditions tested, and did not account for the constitutive resistance of control cortical neurons. Despite de novo induction of IFNs and ISGs in TG neurons in direct response to TLR3 stimulation, HSV-1 triggering of the inducible TLR3-dependent response did not afford protection. Infection in the absence of a preconditioned antiviral state presumably triggered the TLR3 response too late, or to too small a degree due to the limited subtypes of IFNs and ISGs being induced, to prevent incoming virions from delivering their genomes to neuronal nuclei. In contrast, human cortical neurons were more potent: HSV-1 infection triggers a TLR3-dependent response that restricts viral infection in the absence of a preconditioned/induced antiviral state. A primary focus of our research is to decipher the nature of the constitutive TLR3-dependent CNS-intrinsic immunity that operates in cortical neurons and determine its mechanistic underpinnings.

While the present experiments focused on the use of TG neurons for the study of HSE pathogenesis, access to functional TG neurons will facilitate other applications in virology and neurobiology, including the study of herpes labialis, trigeminal zoster, and modeling TG pain of various etiologies. The response of human iPSC-derived TG neurons to nociceptive stimuli was highly robust and occurred in a greater proportion of cells than reported for human iPSC-derived DRG-type nociceptors (13). Recent studies have presented alternative strategies for inducing nociceptive lineages using ectopic expression of transcription factors to directly reprogram fibroblasts into nociceptive neurons (15, 40). However, the robust induction of nociceptors via direct, transcriptional reprogramming has been largely limited to murine cells to date and will require further optimization in human cells. Furthermore, those conditions are not suitable to generate nociceptive lineages with specific regional identity, such as TG neurons. Our data show nociceptive responses of iPSC-derived TG neurons to heat (capsaicin), cold (icilin), and inflammatory (ATP) pain stimuli. Future studies will be required to fully characterize and further manipulate the ability of human iPSC-derived TG neurons to contribute to all nociceptive lineages. The availability of TG neurons can be further used to study their response to nasal and oral toxicants, to screen for toxic side effects of experimental therapeutics on sensory neuron function, to identify candidate therapeutics to prevent or treat sensory neuron damage, and to modulate pain and sensory neuron function. Finally, human iPSC-derived TG neurons may find potential therapeutic applications for direct repair of sensory nerve damage.

Materials and Methods

Human iPSC Generation Using Patient-Derived Fibroblast Cells. Primary fibroblasts from a P554S/E746* ($TLR3^{-/-}$) human patient were reprogrammed using a nonintegrating CytoTune Sendai viral vector kit (Life Technologies), according to protocol 16-I-N139, approved by the Institutional Review Board of the NIH. Primary fibroblasts were plated in 24-well dishes at 50–80% confluency and transduced with the recombinant vectors, according to the manufacturer's protocol. Medium was changed after 24 h of infection and the cells were allowed to grow for 6 d. On day 7, the cells were replated onto mouse embryonic fibroblast feeder cells. Medium was changed to iPSC medium on day 8 and the cells were cultured until colonies formed. Reprogrammed cells were karyotyped to ensure genomic integrity. Fibroblasts have been obtained with patient consent and in accordance to the Helsinki Declaration principles.

Cells and Culture Conditions. The $TLR3^{-/-}$ iPSCs (passage 20–40) (*SI Appendix*, Fig. S6) were the control iPSCs derived either from the fetal fibroblast cell line MRC5 (line J1: XY) (*SI Appendix*, Fig. S1) or from a 9-y-old skin fibroblast donor (line 348, XX). All hiPSC lines were used at passage 15–30 (*SI Appendix*, Fig. S1), as well as the human ESC line H9 [WA-09, female (XX), passage 35–50], were maintained on vitronectin using Essential 8 medium (E8; Fisher Scientific), and passaged twice a week using EDTA (41).

Neural Induction. To induce differentiation, cells were harvested using EDTA (Fisher Scientific) and plated on vitronectin (Fisher Scientific)-coated dishes at a density of 2.5×10^5 cells/cm^2 in E8 + Y-27632 (Tocris Biosciences). After a 24-h attachment phase, differentiation was induced by switching the cells into Essential 6 (E6) medium (Fisher Scientific) (day 0). For generation of cortical neurons, E6 was supplemented with 10 μM SB431542 (Tocris Biosciences), 500 nM LDN193189 (Stem Cell Technologies), and 1 μM XAV939 (Tocris Biosciences) (until day 5). From day 5 on, XAV939 was removed from the medium. Medium was changed every day until day 11. On day 11 cells were passaged 1:3 onto poly-L-ornithine (Sigma), laminin (VWR), and fibronectin (Fisher Scientific) -coated plates in N2 medium supplemented with 10 ng/mL FGF2 (R&D Systems) and 600 nM CHIR99021 (Stemgent) (CHIR concentration was increased after 2 d to 3 μM). Cells were passaged every 3–7 d. Passage 2–3 cells were used to generate frozen stocks, which after quality control were used to further differentiate the cells into cortical neurons.

To generate cortical neurons, frozen neural progenitor cells were seeded onto coverslips or cell-culture plastic pretreated with poly-L-ornithine, fibronectin, and laminin, and differentiated for 14–18 d in neurobasal medium (Fisher Scientific) containing Gibco MEM nonessential amino acids (Fisher Scientific), B-27 supplement (Fisher Scientific), 1 mM L-glutamine (Fisher Scientific), and

10 μM DAPT γ-secretase inhibitor (*N*-[*N*-(3,5-difluorophenacetyl)-L-alanyl]-S-phenylglycine t-butyl ester; R&D Systems). Next, 10 μM Y27632 was used for the initial 24 h after thawing to increase cell survival. Replicate experiments were performed with CNS neurons derived from three independent batches of neural progenitor cells.

For generation of TG neurons, medium on day 0 was supplemented with 10 μM SB431542 and 5 ng/mL BMP4 (R&D Systems) for the first 3 d. From days 2–4, 600 nM CHIR99021 was also added. From day 4 on cells were fed with E6 containing 10 μM SB431542 every other day. Between days 11 and 15, TG placode clusters were either detached using very short trypsin treatment (for freezing a mixed population enriched in TG clusters) or longer trypsin treatment to generate single cells for FACS purification. To produce PNS neurons for use in monitoring progression of HSV-1 infection mixed or FACS-purified TG placode precursors (exact cells used for specific experiments specified above) were seeded onto coverslips or cell culture plastic pretreated as described above. Differentiation was performed in neurobasal medium containing the supplements listed above (for the cortical neurons) as well as 50 ng/mL NGF (PeproTech), 50 ng/mL BDNF (R&D Systems), 50 ng/mL GDNF (PeproTech) (TG neuron maturation medium). Differentiation was achieved over 14–18 d. Replicate experiments were performed with TG neurons derived from three independent batches of differentiated trigeminal placode precursors.

BD Lyoplate Surface Marker Screen. SIX1::H2BGFP cells were differentiated into TG cluster for 12 d. On day 12 of differentiation cells were detached using Accutase and replated as single cells into 96-well plates coated with poly-L-ornithine, laminin, and fibronectin (1.5×10^5 cells per well). After a short attachment phase of 3 h, cells were stained using the BD Lyoplate (BD Biosciences) according to the manufacturer's manual for screening by bioimaging. Cells were analyzed using the Operetta system from PerkinElmer screening the plate for cells coexpressing GFP (SIX1) and Alexa647 (surface antigen). Wells with a high percentage (>20%) of cells coexpressing GFP and Alexa647 in combination with low overall Alexa647 expression (<10%) were defined as positive hits.

Immunocytochemistry and Flow Cytometry. Cells were fixed in 4% PFA, permeabilized using 0.1% Triton-X, and blocked in 10% FCS. Primary antibodies (*SI Appendix*, Table S1) were incubated overnight in 2% FCS at 4 °C. Appropriate Alexa488 or Alexa555 conjugated secondary antibodies were used in combination with nuclear counterstain DAPI. Cells were imaged using and Olympus IX71 inverted microscope. For cell sorting, cells were dissociated using Trypsin and subjected to FACS using either a commercial available GD2 antibody (14.G2a; BD Biosciences, as per the manufacturer's manual) or clinical grade GD2 antibody (3F8, 500 ng/10^6 cells; kind gift from Nai-Kong Cheung, Memorial Sloan Kettering Cancer Center, New York, NY) in combination with an appropriate Alexa647-conjugated secondary antibody. Cells were sorted on a BD FACS Aria III machine.

Quantitative Real-Time PCR. Total RNA was extracted from three consecutive human iPSC-derived TG neuron differentiations using the TRIzol (Fisher Scientific) reagent in combination with Phase-lock tubes (5Prime) according to the manufacturer's protocol. One microgram of total RNA was reverse-transcribed into cDNA using iScript (Bio-Rad). For qRT-PCR we used either the SSoFast EvaGreen Mix (Bio-Rad) in combination with QuantiTect primer assays (Qiagen) on a Bio-Rad CFX Thermal Cycler or Applied Biosystems Assays-on-Demand probe/primer combinations together with a 2× universal reaction mixture, in an ABI PRISM 7700 Sequence Detection System. All reactions were run according to the manufacturer's protocol. Gene expression was either normalized to β-glucuronidase (GUS) or GAPDH. Results are expressed according to the ΔCt method (42).

Calcium Imaging. After etching 40-mm round coverslips with 1N HCL for 10 min, the coverslips were washed and sterilized. After sterilization the coverslips were coated with poly-L-ornithine, laminin and fibronectin, as described previously (43). After GD2 purification by FACS, one drop of cells (5×10^4 cells/10 μL) was plated in the center of the air-dried coverslip. After a 2- to 5-min attachment phase, TG neuron maturation medium was added to the cells. After the indicated time points, calcium imaging was performed as described previously (44). Cells were stimulated with 1 μM capsaicin (Tocris Biosciences), 30 μM ATP (Tocris Biosciences), 1 μM icilin (Tocris Biosciences), or 50 mM KCl (Sigma) for 30 s, respectively. Background readings were subtracted and ratiometric analysis was performed using a customized Matlab (Mathworks) script. The code was also used to identify responding cells. A cell was classified as responding if the change in fluorescence ratio exceeded three times the SDs of the background signal.

Viruses and Infections. HSV1-GS4553, a recombinant of HSV-1 strain F that encodes the mCherry fluorescent protein (45) fused to the pUL25 capsid protein, was previously described (34). HSV1-GS4553 was used for all infections to quantify proportion of infected cells. Differentiated iPSC-derived neurons maintained on coverslips were infected in 1 mL of differentiation media. Because neuronal counts were difficult to determine post-differentiation and the neurons were sparse at the time of infection, multiplicity of infections were not calculated. Instead, infections were carried out using indicated PFU/mL to achieve an equivalent density of input PFU per unit area of coverslip. Cells were scored as infected if they expressed red fluorescence. Specifically, a minimum of 10 fields-of-view were imaged by differential interference contrast microscopy (DIC) and by fluorescence microscopy. For each field captured in this way, neurons were counted in the DIC image and each individual neuron was subsequently scored for red-capsid fluorescence emissions. The aggregate of these data, which consisted of 145–670 neurons per cortical sample and 40–225 neurons per TG sample, was presented as a percent infected value. This procedure was repeated independently to produce three replicas for each sample. Statistical analysis was performed with GraphPad Prism 5.

Live-Cell Imaging. Images of neurons infected with HSV-1 were acquired with an inverted wide-field Nikon Eclipse TE2000-E microscope fitted with a 40 × 1.3 numerical aperture oil objective, and housed in an environmental box maintained at 37 °C (In Vivo Scientific). Images were captured with a CoolSnap HQ2 camera (Photometrics). The MetaMorph software package was used for image acquisition and processing (Molecular Devices). Fluorescence images were captured using 500-ms exposure times.

Cellular Responses to TLR3, HSV-1 Stimulation, and IFN. A synthetic analog of dsRNA [polyinosinic-polycytidylic acid; poly(I:C); InvivoGen] at a concentration of 25 μg/mL or 1,000 IU IFN-β (PeproTech) in 10 μL PBS was added to the neural culture in 1 mL of either PNS or CNS differentiation media 18 h before infection and maintained during infection. In a second subset of experiments, differentiated neurons were pretreated with 2.5 μg/mL recombinant human IL-29/IFN-λ1 (R&D) for 18 h before infection and maintained during infection. To assess the cellular responses to poly(I:C) or HSV-1, FACS-purified TG neuron cultures were stimulated with poly(I:C) for 6 h, or infected with HSV-1 (KOS strain) for 24 h at a multiplicity of 1, cells were collected for RNA extraction and assessed for expression of different IFN subtypes and ISGs by qRT-PCR (see above).

ACKNOWLEDGMENTS. We thank the patients and their families for participating in this study; Dr. Nai-Kong Cheung (Memorial Sloan Kettering Cancer Center) for the 3F8 (clinical grade GD2) antibody; Sanghoon Oh (Memorial Sloan Kettering Cancer Center Molecular Cytology Core) for excellent technical support in calcium imaging experiments and writing of the Matlab code; and Sarah Antinone (Northwestern University) for help with HSV-1 data analysis. The work was funded by NIH Grant R01NS072381. Additional support was provided by NIH Grant R21NS084255, NIH Cancer Center support Grant P30CA008748, Clinical and Translational Science Award program Grant UL1TR001866, Agence Nationale de Recherches Grant IEIHSEER, the Rockefeller University, and INSERM. B.Z. was supported by a NYSTEM postdoctoral fellowship. O.E. received support from the NIH-National Institute of Allergy and Infectious Diseases Immunology and Molecular Pathogenesis Training Program and The American Society for Microbiology Robert Watkins fellowship. L.D.N. is supported by the Division of Intramural Research, National Institute of Allergy and Infectious Diseases, NIH.

1. Roizman B, Whitley RJ (2013) An inquiry into the molecular basis of HSV latency and reactivation. *Annu Rev Microbiol* 67:355–374.
2. Whitley RJ (2006) Herpes simplex encephalitis: Adolescents and adults. *Antiviral Res* 71:141–148.
3. Whitley RJ, et al.; Clinical Assessment (1982) Herpes simplex encephalitis. *JAMA* 247: 317–320.
4. Lafaille FG, et al. (2015) Deciphering human cell-autonomous anti-HSV-1 immunity in the central nervous system. *Front Immunol* 6:208.
5. Kennedy PG (2004) Viral encephalitis: Causes, differential diagnosis, and management. *J Neurol Neurosurg Psychiatry* 75(Suppl 1):i10–i15.
6. Gordon B, Selnes OA, Hart J, Jr, Hanley DF, Whitley RJ (1990) Long-term cognitive sequelae of acyclovir-treated herpes simplex encephalitis. *Arch Neurol* 47:646–647.
7. Bereczky-Veress B, et al. (2008) Host strain-dependent difference in susceptibility in a rat model of herpes simplex type 1 encephalitis. *J Neurovirol* 14:102–118.
8. Johnson RT, Mims GA (1968) Pathogenesis for viral infections of the nervous system. *N Engl J Med* 278:84–92.

9. Takahashi K, et al. (2007) Induction of pluripotent stem cells from adult human fibroblasts by defined factors. *Cell* 131:861–872.
10. Yu J, et al. (2007) Induced pluripotent stem cell lines derived from human somatic cells. *Science* 318:1917–1920.
11. Cherry AB, Daley GQ (2013) Reprogrammed cells for disease modeling and regenerative medicine. *Annu Rev Med* 64:277–290.
12. Osakada F, Takahashi M (2011) Neural induction and patterning in Mammalian pluripotent stem cells. *CNS Neurol Disord Drug Targets* 10:419–432.
13. Chambers SM, et al. (2012) Combined small-molecule inhibition accelerates developmental timing and converts human pluripotent stem cells into nociceptors. *Nat Biotechnol* 30:715–720.
14. Fattahi F, et al. (2016) Deriving human ENS lineages for cell therapy and drug discovery in Hirschsprung disease. *Nature* 531:105–109.
15. Wainger BJ, et al. (2015) Modeling pain in vitro using nociceptor neurons reprogrammed from fibroblasts. *Nat Neurosci* 18:17–24.
16. Hoelting L, et al. (2016) Stem cell-derived immature human dorsal root ganglia neurons to identify peripheral neurotoxicants. *Stem Cells Transl Med* 5:476–487.
17. Edvinsson L (2017) The trigeminovascular pathway: Role of CGRP and CGRP receptors in migraine. *Headache* 57:47–55.
18. Casrouge A, et al. (2006) Herpes simplex virus encephalitis in human UNC-93B deficiency. *Science* 314:308–312.
19. Zhang SY, et al. (2007) TLR3 deficiency in patients with herpes simplex encephalitis. *Science* 317:1522–1527.
20. Sancho-Shimizu V, et al. (2011) Herpes simplex encephalitis in children with autosomal recessive and dominant TRIF deficiency. *J Clin Invest* 121:4889–4902.
21. Herman M, et al. (2012) Heterozygous TBK1 mutations impair TLR3 immunity and underlie herpes simplex encephalitis of childhood. *J Exp Med* 209:1567–1582.
22. Lim HK, et al. (2014) TLR3 deficiency in herpes simplex encephalitis: High allelic heterogeneity and recurrence risk. *Neurology* 83:1888–1897.
23. Andersen LL, et al. (2015) Functional IRF3 deficiency in a patient with herpes simplex encephalitis. *J Exp Med* 212:1371–1379.
24. Zhang SY, et al. (2013) TLR3 immunity to infection in mice and humans. *Curr Opin Immunol* 25:19–33.
25. Lafaille FG, et al. (2012) Impaired intrinsic immunity to HSV-1 in human iPSC-derived TLR3-deficient CNS cells. *Nature* 491:769–773.
26. Tchieu J, et al. (2017) A modular platform for differentiation of human PSCs into all major ectodermal lineages. *Cell Stem Cell* 21:399–410.e7.
27. Dincer Z, et al. (2013) Specification of functional cranial placode derivatives from human pluripotent stem cells. *Cell Rep* 5:1387–1402.
28. McCabe KL, Sechrist JW, Bronner-Fraser M (2009) Birth of ophthalmic trigeminal neurons initiates early in the placodal ectoderm. *J Comp Neurol* 514:161–173.
29. Vincent M, Thiery JP (1984) A cell surface marker for neural crest and placodal cells: Further evolution in peripheral and central nervous system. *Dev Biol* 103:468–481.
30. Zimmer B, et al. (2016) Derivation of diverse hormone-releasing pituitary cells from human pluripotent stem cells. *Stem Cell Rep* 6:858–872.
31. Yuan SH, et al. (2011) Cell-surface marker signatures for the isolation of neural stem cells, glia and neurons derived from human pluripotent stem cells. *PLoS One* 6: e17540.
32. Marmigère F, Ernfors P (2007) Specification and connectivity of neuronal subtypes in the sensory lineage. *Nat Rev Neurosci* 8:114–127.
33. Guo Y, et al. (2011) Herpes simplex virus encephalitis in a patient with complete TLR3 deficiency: TLR3 is otherwise redundant in protective immunity. *J Exp Med* 208: 2083–2098.
34. Huffmaster NJ, Sollars PJ, Richards AL, Pickard GE, Smith GA (2015) Dynamic ubiquitination drives herpesvirus neuroinvasion. *Proc Natl Acad Sci USA* 112:12818–12823.
35. Smith G (2012) Herpesvirus transport to the nervous system and back again. *Annu Rev Microbiol* 66:153–176.
36. Picard C, et al. (2018) International Union of Immunological Societies: 2017 Primary Immunodeficiency Diseases Committee Report on inborn errors of immunity. *J Clin Immunol* 38:96–128.
37. Bousfiha A, et al. (2018) The 2017 IUIS phenotypic classification for primary immunodeficiencies. *J Clin Immunol* 38:129–143.
38. Rosato PC, Leib DA (2014) Intrinsic innate immunity fails to control herpes simplex virus and vesicular stomatitis virus replication in sensory neurons and fibroblasts. *J Virol* 88:9991–10001.
39. Song R, et al. (2016) Two modes of the axonal interferon response limit alphaherpesvirus neuroinvasion. *MBio* 7:e02145-e15.
40. Blanchard JW, et al. (2015) Selective conversion of fibroblasts into peripheral sensory neurons. *Nat Neurosci* 18:25–35.
41. Chen G (2008) *Splitting hESC/hiPSC Lines with EDTA in Feeder Free Conditions* (StemBook, Cambridge, MA).
42. Schmittgen TD, Livak KJ (2008) Analyzing real-time PCR data by the comparative C(T) method. *Nat Protoc* 3:1101–1108.
43. Steinbeck JA, et al. (2016) Functional connectivity under optogenetic control allows modeling of human neuromuscular disease. *Cell Stem Cell* 18:134–143.
44. Calder EL, et al. (2015) Retinoic acid-mediated regulation of GLI3 enables efficient motoneuron derivation from human ESCs in the absence of extrinsic SHH activation. *J Neurosci* 35:11462–11481.
45. Shaner NC, et al. (2004) Improved monomeric red, orange and yellow fluorescent proteins derived from *Discosoma* sp. red fluorescent protein. *Nat Biotechnol* 22: 1567–1572.